HEFAT2014
10th International Conference on Heat Transfer, Fluid Mechanics and Thermodynamics
14 – 16 July 2014
Orlando, Florida

DISH STIRLING CAVITY/RECEIVER: THERMAL MODEL AND DESIGN OPTIMIZATION

C. Monné*, R. Gil, M. Muñoz, F. Moreno

*Author for correspondence
Engineering and Architecture School, Mechanical Engineering Department,
Universidad de Zaragoza,
Zaragoza, 50018,
Spain,
E-mail: cmmb@unizar.es

ABSTRACT

This paper presents a thermal model for a dish Stirling cavity. Finite differences method has been applied to develop this theoretical model that enables the cavity efficiency optimization quantifying conduction, convection and radiation heat exchange. View factors of all surfaces involved have been calculated accurately to resolve the radiosity method. The model has been implemented in a tool that enables to vary receiver dimensions and materials in order to determine the optimal cavity design. Using this developed tool, there have been found some results that lead to an optimal cavity; regarding material properties, receiver absorptivity presents the biggest influence in cavity performance; and regarding geometry parameters, aperture ratio presents the biggest influence and aperture height shows an optimal value different from one to another aperture ratio.

INTRODUCTION

Nowadays, the Stirling dish is a device in progress. It produces electricity using concentrated solar thermal energy to drive a Stirling engine. This system uses a parabolic mirror (with dual axis tracking) to concentrate solar radiation onto a receiver, which handles energy levels extremely high; this receiver is integrated in the Stirling engine, being it's function to heat the working fluid.

The Stirling dish receiver absorbs thermal energy from a concentrator whose concentration ratio can reach up to 13000 suns. Consequently, losses in this part must be known and controlled, since they may entail the difference between a profitable and an unprofitable Stirling dish.

This situation practically requires the study of the cavity behaviour as a function of geometry and materials. Three different kinds of losses are involved in the receiver solar dish; conduction, convection and radiation, and all of them have been studied in many papers.

On the subject of radiation losses, ray tracing methods (using algorithms based on the MonteCarlo Statistic method) have been widely used by many authors in order to model thermal systems [1] [2] and to predict radiation performance [3]. Instead of that procedure, another way to resolve a thermal model exists, and it is the radiosity method, applied in some studies to analyse a unique geometry [4][5], or several geometries [6], assuming semi-gray radiation problem and diffuse surfaces on fixed geometries.

NOMENCLATURE

A	[m^2]	*Area*
Ec	[-]	Cavity emission spectrum (thermal radiation)
Es	[-]	Solar emission spectrum (solar radiation)
F	[-]	View factor
H	[cm]	Interior cavity height
J	[W/ m^2]	Radiosity
R	[cm]	Radius
T	[K]	Temperature

Special characters

α	[-]	Absorptivity
δ	[m]	Height between dish 1 and dish 2 to evaluate F_{d1d2} calculation
ε	[-]	Emissivity
η	[-]	Performance
λ	[m]	Wavelength
ρ	[-]	Reflectivity
σ	[W/(m^2K^4)]	Steffan-Boltzmann constant (=5,6696 x 10^{-8})
φ	[W/m^2]	Incident solar flux

Subscripts

ap	Aperture
d1	Dish 1 to evaluate F_{d1d2} calculation
d2	Dish 2 to evaluate F_{d1d2} calculation
i	Surface "i"
j	Surface "j"

The main disadvantage of ray-tracing methods is the large computation time needed to solve the problem. Radiosity method requires a simpler equation system.

Regarding convection losses, some authors have studied the influence of inclination, temperature and wind velocity; finding out a stagnant zone [7] that increases its value when inclination is near to 90° [8], and wind speed and direction present a determinate range of values [9] that improve the cavity efficiency.

This work presents a thermal model based on the radiosity method to evaluate radiation losses; and convection losses are calculated from a convective coefficient and an interior and exterior fluid temperature whose values are defined according to the literature. These facts are assessed applying the finite difference method using EES software [10]. The main original contribution of this thermal model is the cavity surface division; it is divided into a number of surfaces calculated from the introduced dimensions (variable) and a precision input, and consequently, all view factors are calculated accurately using theoretical rules. In addition, solar energy source (that has been modelled as non-uniform) and material properties can be varied in the model.

The aim of this work is to optimize the cavity efficiency studying different situations of convection, solar incoming energy, materials, and geometry.

THERMAL MODEL

This work has been developed starting from a basic cavity, shown in **Figure 1**. Energy radiation coming from the concentrator enters the cavity through the opened area, and leaves the cavity through the absorber, the closed area integrated with the Stirling engine. The cavity must be designed in order to get the most similar quantity of energy leaving the cavity towards Stirling engine, and leaving the concentrator towards the cavity. To get it, this cavity presents a second reconcentrator zone (upper space with different inclination to diminish the spillage losses). This thermal model assumes cylindrical symmetry, and gray and diffuse surfaces.

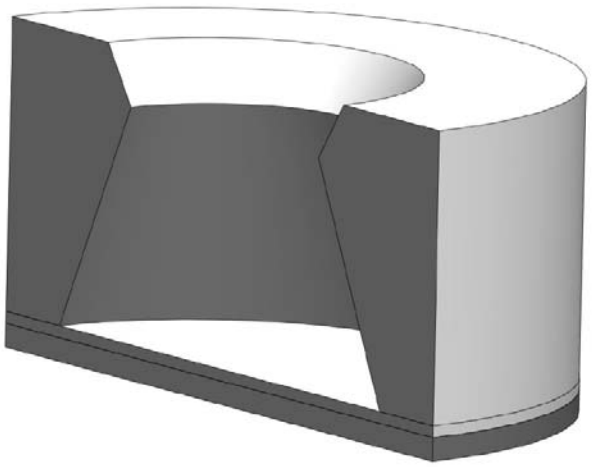

Figure 1 Modelled cavity geometry

Finite Differences

The expressions to apply the finite differences method are obtained from an energy balance in the finite volume of each one of the nodes that comprise the element to study, so it is necessary to know each one of the heat contributions in all different cavity zones.

An interior node presents conduction heat transfer, while a node belonging to the cavity border presents, in addition to conduction, convection and radiation heat exchange. Conductive and convective heat exchange are resolved using Fourier's Law and Newton's Law of Cooling respectively (setting convective coefficient as commented previously).

Discretization

The discretization to resolve the finite difference method in this model could be characterized as dynamic. The number of nodes depends on the dimensions of the cavity and the precision variable, being the area of each one of the nodes different from the rest of nodes defining the cavity volume. Despite this circumstance, a calculation pattern is established due to the existence of some zones (composed by a different number of nodes in each simulation) that present similar boundary conditions.

Figure 2 shows the finite volumes of a discretization applying cylindrical symmetry in a particular simulation.

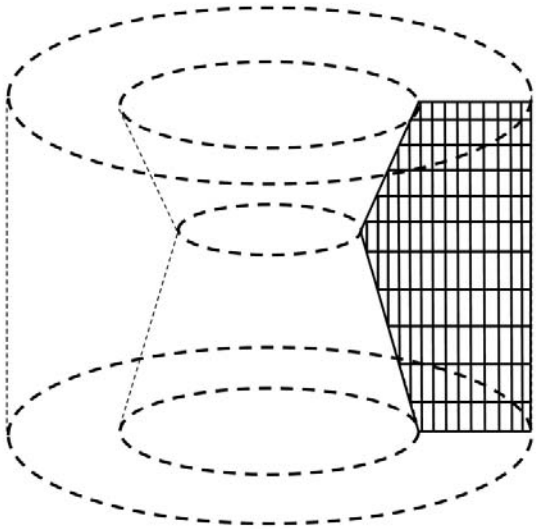

Figure 2 Cavity discretization (finite volumes)

Solar Energy Source

Experimental studies show that concentrator focuses more energy in the centre of the receiver [4]; because of this reason, solar flux distribution has been modelled as a central circle and some crown circles receiving a different level of incoming energy quantity (as shows **Figure 3**). Cylindrical symmetry is an approximation considered to be right.

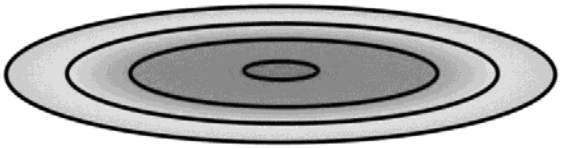

Figure 3 Incoming solar energy distribution

Radiation Exchange

Radiation exchange has been calculated considering two different bands in electromagnetic spectrum. One of those bands refers to short wavelength (λ<3μm, solar radiation emitted from the Sun at about 5770 K), and the other one refers to long wavelength (λ>3μm, thermal radiation emitted at about 1000 K). This procedure has been adopted and validated previously [4], considering independent phenomena (short and long wavelength) and adding their contributions.

In the following, "es" refers to solar radiation band, and "ec" refers to thermal radiation band. "Ec" spectrum affects complete cavity, and "es" only affects the lower volume of the cavity when the spillage losses are negligible.

Figure 4 shows different cavity zones; zone 1 has been modelled as a connection between upper and lower volume of the cavity, and it is the plane where reflected energy leaves the cavity; zone 2 division rings represent different incoming energy levels, and beneath it, it is the absorber; zone 3 corresponds to lateral cavity surface; and finally zone 4 has been modelled as a black body at environment temperature.

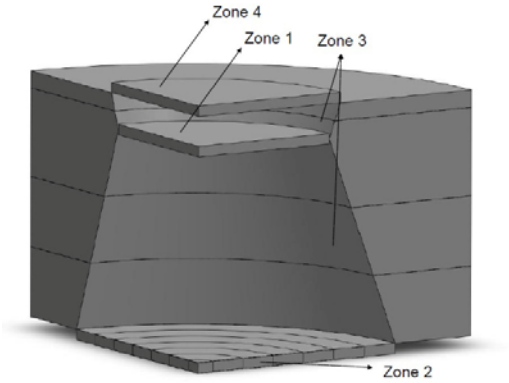

Figure 4 Different cavity zones

As it has been previously explained, "es" and "ec" spectrum have been calculated as independent phenomena; when zone 1 belongs to "es" spectrum, similar division rings to zone 2 have been considered to be able to analyze different energy levels in this plane if necessary. Zone 1, zone 2 and zone 3 compose "es" spectrum calculation when spillage is negligible; and all zones compose "ec" spectrum calculation.

The next equations are used to solve radiation heat exchange:

$$q_{1\to 2} = A_1 \cdot F_{12} \cdot (J_1 - J_2) \quad (1)$$

$$J_i = J_{es_i} + J_{ec_i} \quad (2)$$

$$J_{ec_i} = \varepsilon\sigma {T_i}^4 + \rho \sum_j F_{ji} \left(J_{ec_j} - J_{ec_i}\right) \quad (3)$$

$$J_{es_i} = \rho_i \left(\varphi_i + \sum_j F_{ij} \cdot J_{es_j}\right) \quad (4)$$

These previous expressions form a dynamic equation system composed of a different surfaces number, and consequently a different equations and variables number depending on geometry and precision set by user. This work's simulations consider a lateral surfaces number between 50 and 150 where each node must be evaluated carefully in order to consider all heat contributions.

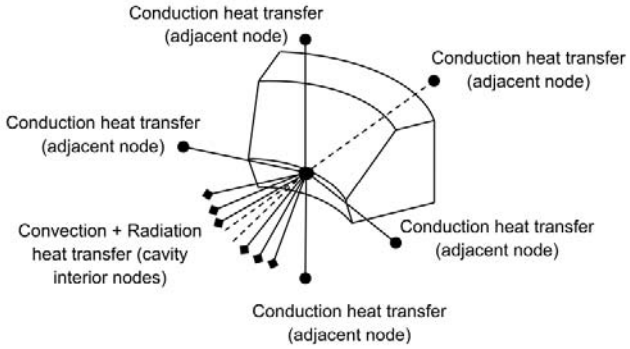

Figure 5 Heat contributions to a cavity border node

Figure 5 shows the node between upper and lower lateral cavity surface, and it shows all heat contributions (including radiation heat transfer exchanged with a changing number of nodes depending on the simulation).

View Factors

Due to the dynamic equation system proposed, it becomes necessary to calculate a different a view factor quantity when geometry and precision variable change. Each surface division has a different area, and this area can change from one to another simulation.

Radiation equations are posed on all surfaces, and due to the discretization, some peculiarities must be considered; **Figure 5** shows an example where it is illustrated all different view factors to calculate from each one of the surfaces that constitute the lateral cavity surface.

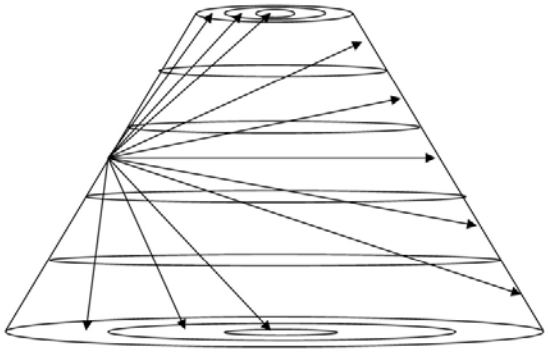

Figure 6 Different view factors from a lateral surface

Each one of the different arrows in **Figure 6** refers to a view factor that must be calculated using a characteristic pattern. Particular or characteristic calculation patterns quantity increases considering all cavity nodes and not only one as it is shown in **Figure 6**, which ends whit a complex calculation system.

The developed process to carry out this calculation system has been based on three view factor basic laws:

- Sum law:
$$\sum_j F_{ij} = 1 \quad (5)$$

- Reciprocity law:
$$A_1 F_{12} = A_2 F_{21} \quad (6)$$

- View factor between two coaxial and parallel dishes [11]:
$$F_{d1d2} = \frac{1}{2}\left\{X - \left[X^2 - 4\left(\frac{x_{d2}}{x_{d1}}\right)^2\right]^{1/2}\right\} \quad (7)$$
$$x_{d1} = \frac{R_{d1}}{\delta},\ x_{d2} = \frac{R_{d2}}{\delta},\ X = 1 + \frac{1+{x_{d2}}^2}{{x_{d1}}^2} \quad (8)$$

Besides these rules, regarding lateral surfaces, the view factor from each one to itself is different from 0 because of its concave shape.

CAVITY OPTIMIZATION

The developed tool has been used in order to find an optimal cavity varying material properties and cavity dimensions. Cavity simulations have been carried out considering 28 kWt of total energy input, which is the required power to get approximately 10 kWe (Cleanergy's Stirling engine C11S [12]). The cavity optimization has been carried out in order to find the best thermal efficiency, defined as the ratio between energy transmitted to Stirling engine and energy received from the parabolic concentrator. Simulations presented in this section study a cavity parameter (material or dimension) being the rest fixed (**Table 1** shows their values while not changing in order to be studied for optimization).

Table 1 Fixed properties and parameters to simulate.

Material Properties	
Cavity Absorptivity [-]	0,965
Absorber Absorptivity [-]	0,834
Cavity Emissivity [-]	0,917
Absorber Emissivity [-]	0,73
Cavity Conductivity [W/mK]	0,005
Equivalent Convection Coefficient [W/m^{2}K]	6
Equivalent Interior Air Temperature [K]	600
Environment Temperature [K]	298
Geometrical Parameters	
Reconcentrator Radius [cm]	13,28
Aperture Radius [cm]	10,13
Receiver Radius [cm]	15,98
External Cavity Radius [cm]	25,43
Aperture Height [cm]	12,86
Cavity Height [cm]	15

When aperture radius is studied, material properties and receiver radius are those shown in **Table 1**, but some geometrical parameters are different. Reconcentrator radius is considered 3 cm larger than aperture radius, and cavity height is 4 cm larger than aperture height (whose value is 9,66 cm).

When aperture height is studied, material properties, aperture radius and receiver radius are those shown in **Table 1**, and reconcentrator radius and cavity height are considered equal to aperture radius study.

Material Properties Optimization

Studying losses due to material properties, receiver absorptivity has been determined as the most important property to be controlled in order to get the best thermal efficiency. **Figure 7** shows how performance increases nearly 20 % while varying receiver absorptivity along its entire possible range of variation.

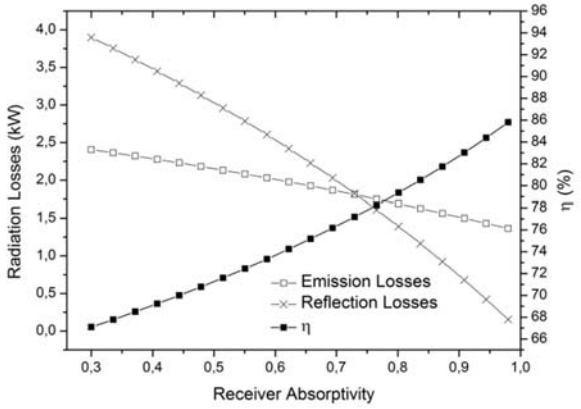

Figure 7 Efficiency and radiation losses varying receiver absorptivity (solar source: 28 kWt)

Increasing receiver absorptivity, reflection losses decrease a great deal; Stirling engine receives much more energy, and consequently less energy is reflected to cavity, decreasing cavity temperature and emission losses.

When cavity absorptivity is varied, emission and reflection losses show different behaviour, but the total effect on losses is practically zero. If cavity absorptivity shows an increment, energy staying in the cavity increases, and consequently less energy is reflected and cavity temperature increases. Due to the temperature augment on cavity surface, emission losses increase. **Figure 8** shows this particular behaviour.

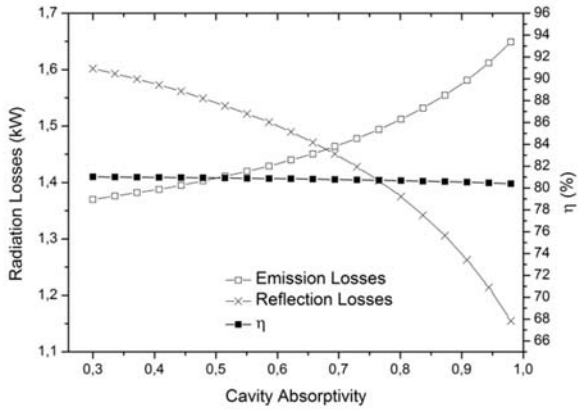

Figure 8 Efficiency and radiation losses varying cavity absorptivity (solar source: 28 kWt)

Emissivity variation produces a negligible effect on losses, and consequently, on cavity thermal performance. This behaviour denotes the minor importance of "ec" spectrum.

Regarding conduction losses, **Figure 9** shows a logarithmic relationship between them and conduction coefficient.

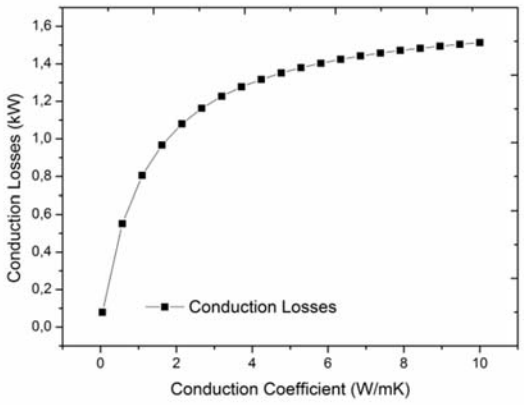

Figure 9 Conduction losses varying conduction coefficient (solar source 28 kWt)

Cavity Geometry Optimization

In order to find an optimal geometry, two strategies have been carried out; **Figure 10** shows how cavity aperture is varied, and **Figure 11** shows how cavity height is varied in these simulations. Using the same criteria to materials optimization, there have been fixed variables not in study in each one of the simulation. To study cavity aperture optimization, absorber radius does not change its value, and reconcentrator radius preserves its relationship to aperture radius; and to study cavity height, all radius and reconcentrator height have been fixed.

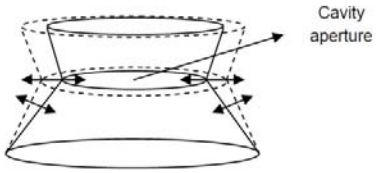

Figure 10 Cavity aperture radius variation

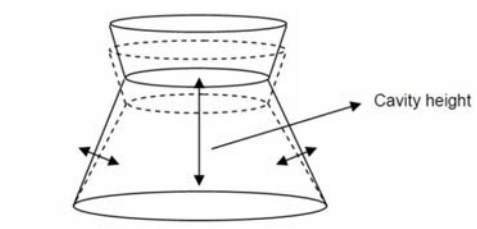

Figure 11 Cavity height variation

Figure 12 shows how radiation losses decrease when aperture radius does. This behaviour is completely logical due to the increment of reflections and the decrease of energy leaving the cavity to the environment; being the concentrator and its optical characteristics the designing responsible of this aperture radius value.

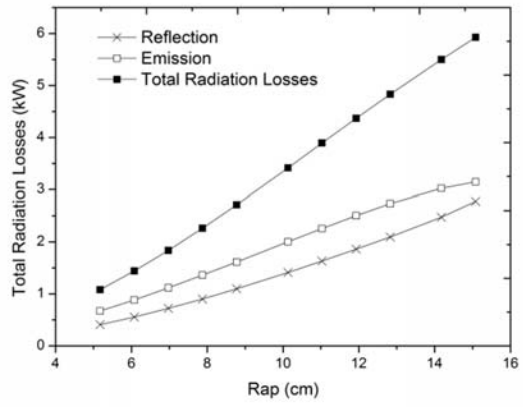

Figure 12 Radiation losses varying aperture radius (solar source 28 kWt)

Consequently, knowing the limitations due to optical properties of the concentrator and the relationship between aperture radius and performance, obtained using the developed tool, it can be obtained the optimal aperture ratio. **Figure 13** shows how performance varies when aperture radius does.

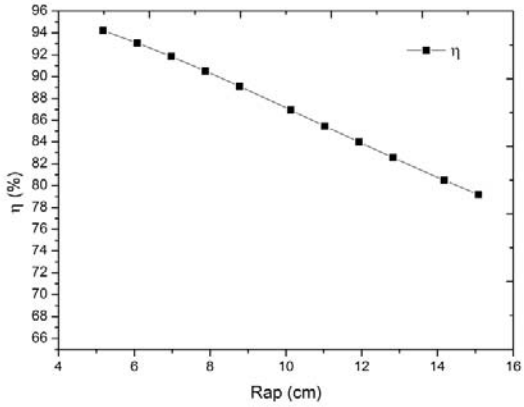

Figure 13 Efficiency varying aperture radius (solar source: 28 kWt)

Once aperture ratio has been determined, cavity height influence in the efficiency is studied. **Figure 14** show how efficiency increases up to an optimal height value; if height increases more than that threshold value, efficiency decreases. This tendency is repeated considering different operation cavity conditions and aperture ratio values.

Designing the best cavity in terms of thermal efficiency, the first step must be the aperture ratio determination (due to its higher influence), and the second step must be the cavity height determination (lower influence in thermal efficiency).

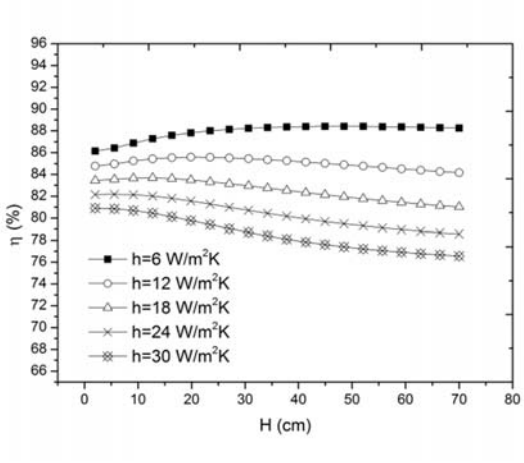

Figure 14 Efficiency varying cavity height (solar source: 28 kWt)

Finally, conduction losses show an exponential behaviour when varying cavity thickness; a little value of this parameter can be critical declining cavity performance, but making it larger than 50 % of absorber radius, thermal efficiency is hardly improved.

CONCLUSIONS

A thermal model based on the finite differences method has been presented. Conduction, convection and radiation losses have been evaluated; being the last calculated using the radiosity method and developing a complex procedure to obtain all necessary view factors (amount depending on the dimensions an resolution precision).

Using this model, a tool that enables the cavity optimization and can be useful to guide the cavity design has been created. As conclusions, the absorber absorptivity is the material property that presents the higher influence on thermal efficiency; regarding cavity dimensions, aperture radius shall be the smallest (limited by concentrator optical characteristics), and cavity height should be selected depending on that aperture radius to improve thermal efficiency taking advance of the optimal value detected by means of this model.

REFERENCES

[1] Müller R., Steinfeld A., Band-approximated radiative heat transfer analysis of a solar chemical reactor for the thermal dissociation of zinc oxide, *Solar Energy*, Vol. 81, October 2007, pp. 1285-94

[2] Shuai Y., Xia X.L., Tan H.P., Radiation performance of dish solar concentrator/cavity receiver systems, *Solar Energy*, Vol. 82, January 2008, pp. 13-21

[3] Li Z., Tang D., Du J., Li T., Study on the radiation flux and temperature distributions of the concentrator-receiver system in a solar dish/Stirling power facility, *Applied Thermal Engineering*, Vol. 31, July 2011, pp. 1780-9

[4] Nepveu F., Ferriere A., Bataille F., Thermal model of a dish/Stirling systems, *Solar Energy*, Vol. 83, January 2009, pp. 83-89

[5] Montiel Gonzalez M., Hinojosa Palafox J., Estrada C.A., Numerical study of heat transfer by natural convection and surface thermal radiation in an open cavity receiver. *Solar Energy*, Vol. 86, April 2012, pp. 1118-28

[6] Natarajan S.K., Reddy K.S., Mallick T.K., Heat loss characteristics of trapezoidal cavity receiver for solar linear concentrating system, *Applied Energy*, Vol. 93, May 2012, pp. 523-531

[7] Prakash M., Kedare S.B., Nayak J.K., Determination of stagnation and convective zones in a solar cavity receiver, *International Journal of Thermal Sciences*, Vol. 49, April 2010, pp. 680-691

[8] Wu S.Y., Xiao L., Cao Y., Li Y.R., Convection heat loss from cavity receiver in parabolic dish solar thermal power system: A review, *Solar Energy*, Vol. 84, August 2010, pp. 1342-1355

[9] Xiao L., Wu S.Y., Li Y.R., Numerical study on combined free-forced convection heat loss of solar cavity receiver under

wind environments, *International Journal of Thermal Sciences*, Vol. 60, October 2012, pp. 182-194
[10] F-Chart Software, LCC. Engineering Equation Solver.
[11] Incropera FP, DeWitt DP. Fundamentals of Heat and Mass Transfer. 4th ed. John Willey & Sons; 1996.
[12] Cleanergy, 2013 <http://www.cleanergy.com/> (accessed 14.10.13)